Analysis of the influence of phreatic surface position on the deformation of fill slope by using 1G shaking table tests

Hidehiko MURAO[1] and Kentaro NAKAI[1]

[1] Department of Civil Engineering, Nagoya University, Furocho, Chikusa, Nagoya City, Japan.

ABSTRACT

Seismic behavior of the fill slope naturally differs depending on the phreatic surface position. In this paper, 1G shaking table tests of unsaturated fill slopes were conducted to understand the influence of the phreatic surface position through the comparison with saturated condition. The experimental results showed that although the failure mechanism in which the slip surface is formed by the reduction in rigidity is common, the input acceleration at failure and deformation mode are different. When the slip surface is formed and failure occurs, the input acceleration in the unsaturated fill slope is larger and the deformation at same excitation stage is small.

Keywords: slope stability; phreatic surface; unsaturated condition; seismic response analysis; failure mode

1 INTRODUCTION

In Japan, approximately 73% of the national land is mountainous with a limited flat terrain. Hence, the hilly areas are leveled, and the soil generated is utilized to form embankments in a nearby valley or low-lying area. However, these fill slopes are a geotechnical risk factor during the event of an earthquake, and many serious damages due to major earthquakes have been reported (Kamai et al. 2013). To construct fill slopes that are difficult to deform during earthquakes, strict compaction management is proposed, and it is considered to be effective for seismic design. However, in the Noto Peninsula earthquake that occurred in 2007, a large-scale landslide occurred on the fill slope on Noto toll road, which was presumed to be a high quality and well-compacted embankment. Therefore, a precise aseismic design method capable of withstanding major earthquakes, is required (Nakano et al., 2010). Until now, various studies have been conducted on designing such a method, however, there are still many unknowns in the complicated deformation/failure behavior of the fill slopes during an earthquake.

To understand the deformation/failure mechanism of the fill slopes in the event of an earthquake, authors have performed the 1G shaking table tests of saturated fill slopes (Murao et al., 2018). The results showed that the deformation/failure mechanism of a fill slope cannot be defined by only one sliding surface. Multiple sliding surfaces are progressively formed depending on the ground and external conditions. Moreover, evaluating the seismic stability of fill slopes depends not only on the magnitude of the acceleration but also on the relationship between the natural frequency of the fill slope and input frequency. These phenomena were not considered in the seismic-intensity method or Newmark's method used in the conventional design.

Many influence factors on the seismic stability of the fill slope exist in addition to the frequency characteristics. For example, the phreatic surface position of the fill slope always fluctuates owing to groundwater supply from the posterior slope and rainfall, and the seismic behavior of the fill slope naturally differs depending on the phreatic surface position. In this paper, 1G shaking table tests of unsaturated fill slopes were conducted to understand the influence of the phreatic surface position on the fill-slope stability through the comparison with previous results of saturated condition (Murao et al. 2018).

2 PREPARATION OF THE MODEL SLOPE

As shown in Fig. 1, seven accelerometers (ch.1 to ch.6 and ch.8) and seven pore water pressure meters (ch.9 to ch.15) were embedded into the embankment during its construction, and one accelerometer (ch.7) was installed on the bottom of the soil tank to measure the input excitation. The shape of the bedrock and embankment were assumed the same as that of a typical fill slope, which is formed by the combination of leveling and banking. Table 1 and Fig. 2 list the physical properties of embankment material. The bedrock part was required to be harder and with a much higher strength than the embankment part. Therefore, the bedrock part was prepared by adding
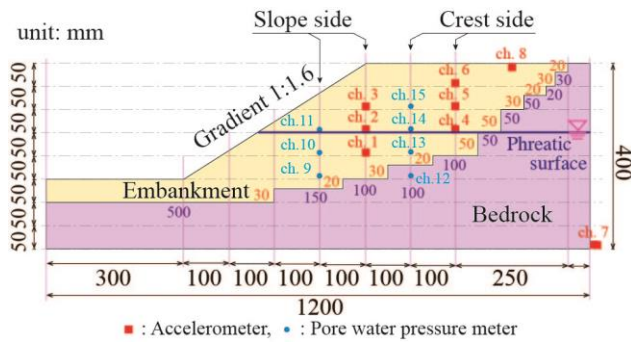
Fig. 1 Cross section of the model slope

Table 1 Physical properties of embankment material

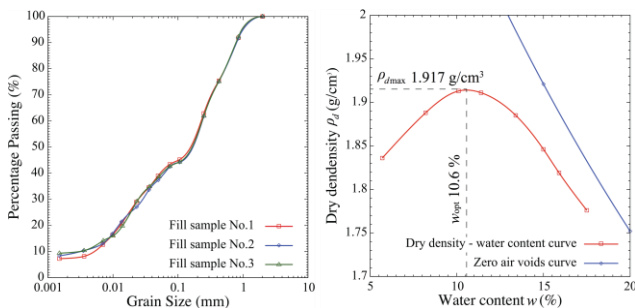| Soil particle density ρ_d (g/cm^3)	2.698
Clay fraction (%)	14.7
Silt fraction (%)	28.2
Fine fraction (%)	32.3
Medium sand (%)	16.7
Coarse sand (%)	8.1

Fig. 2 Physical properties of embankment material

cement-solidification material at a rate of 150 kg/m^3 to the one in which a fine fraction of the embankment material was removed. Seepage was induced in the model slope by using a water tank at the front and rear of the soil tank. As we considered an unsaturated fill slope in this experiment, water was supplied so that a phreatic surface was formed at the center of the embankment part (with a crest of 15 cm). An acrylic plate was provided on the side of the soil tank to observe the deformation.

The sweep test separately performed on the model slope showed that the natural frequency of the model slope before excitation was approximately 50 Hz for both saturated and unsaturated conditions. Input frequency is assumed to be 50 Hz as in the past research. Regarding the excitation condition, it is the same as the past research (Murao et al., 2018).

3 RESULT AND DISCUSSION

3.1 Difference in deformation mode

Figures 4 and 5 show the side views of the saturated (Case A) and unsaturated (Case B) fill slopes before and after excitation (with input accelerations of 5.2 and 8.2 m/s^2), respectively. The slip surfaces shown in Figs. 4 and 5 were determined from the displacements of the markers installed on the side surface and from the change in the amplification factor and pore water

pressure behavior, as described later in the text.

In Case A (saturated condition), when the input acceleration reached 1.2 m/s^2, the pore water began to discharge from the slope surface and crest. Eventually, when the input acceleration reached 4.2 m/s^2, an open crack was generated in the ground surface and a shallow slip can be clearly seen. Furthermore, the open crack became clearly visible with the increase in the excitation level. Moreover, when the input acceleration reached 5.7 m/s^2, a deep slip occurred from the crest of the embankment toward the toe of the slope and a large settlement occurred at the crest. Thus, in case of a saturated fill slope, the slip failure gradually propagates from the ground surface to a deeper part, and eventually caused a complete failure.

Figure 6 shows the top view (crest and slope surface) of the input acceleration stage of (a) 3.2m/s^2, (b) 5.7m/s^2, and (c) 8.2m/s^2 of Case B. When the input acceleration reached 3.2 m/s^2, pore water started discharging from the slope surface (Fig. 6 (a)). This differs from Case A in that the excitation stage at the start of the pore water discharge is large, and it occurs only from the lower part of the slope. The place/level of pore water discharge corresponds exactly or slightly higher to the position of the phreatic surface position. As the excitation stage increased, small cracks began appearing at the discharged portion, and when the input acceleration reached 5.7 m/s^2, cracks gradually became clear and open (Slip surface 1 in Fig. 5). The slip surface was pushed toward the side of the slope starting from the position of the phreatic surface, and the head of soil mass gradually deformed and collapsed. Although the pore water discharge at the crest was still not observed, large open cracks were observed to penetrate the crest when input acceleration reached 8.2 m/s^2, as shown in Fig. 6 (c) (Slip surface 3 in Fig. 5). The result of the occurrence of large cracks and lateral displacements near the top of the slope is consistent with the damage report of major earthquakes illustrated in Fig. 7. In the case of an unsaturated fill slope, the slope surface is pushed out laterally so that the slip or open crack gradually develops backwards.

The comparison of the saturated (Case A) and unsaturated (Case B) conditions shows that the deformation mode is different, and the acceleration level when the unsaturated fill slope shows failure is larger than for the saturated fill slope. This implies that the lower groundwater level has higher earthquake stability. These results indicate that the groundwater drainage is effective as an earthquake-resistant measure.

3.2 Relationship between acceleration amplification factor and excess pore water pressure

Relationship between acceleration amplification factor and excess pore water pressure The acceleration
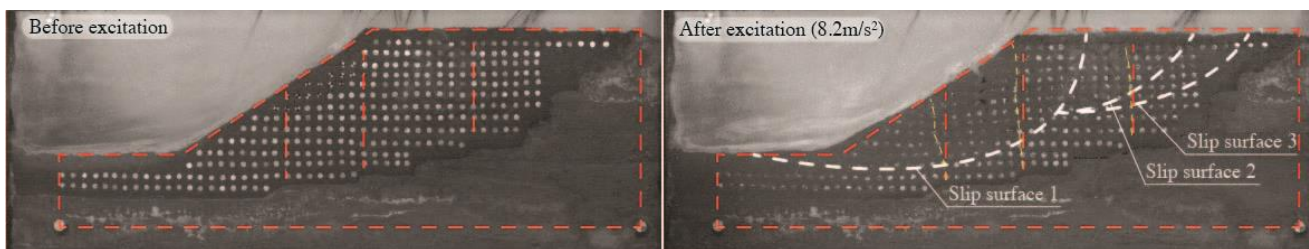
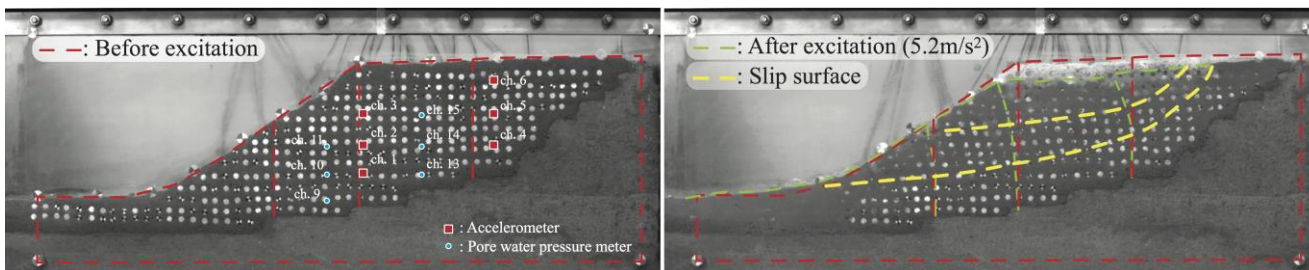Fig. 4 Side view of the model before and after excitation of Case A.

Fig. 5 Side view of the model before and after excitation of Case B.
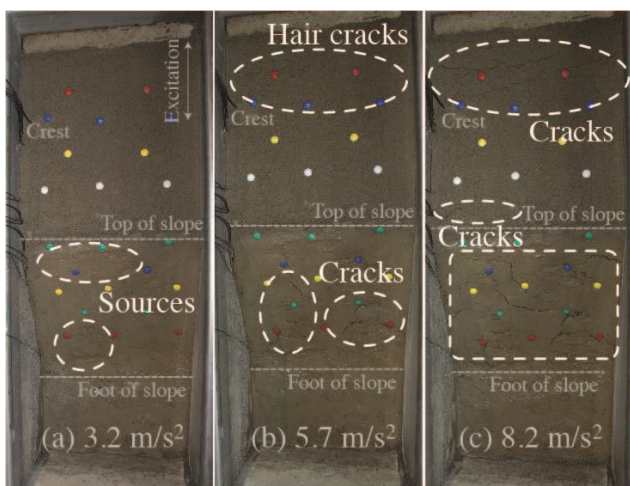

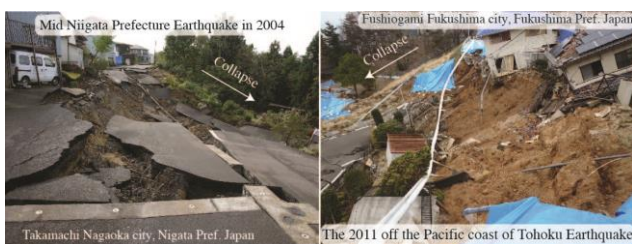Fig. 6 Changes of the upper part of the embankment by excitation

Fig. 7 Collapse of the fill slope from the embankment slope

amplification factor (hereafter referred to as the amplification factor) was defined as the ratio of the amplified acceleration (observed acceleration at the crest) to the input acceleration, as shown in Eq. (1).

$$\text{Amplification factor} = \frac{\text{Amplified acceleration}}{\text{Input acceleration}} \quad (1)$$

Figures 8 and 9 show the change in the amplification factor and excess pore water pressure of Case B, respectively. The comparison of the amplification factors in the depth direction shows that in the initial stage, amplification is higher at positions close to the ground surface with the following relationship: ch.1 (lower) < ch.2 (middle) < ch.3 (upper), ch.4 (lower) < ch.5 (middle) < ch.6 (upper). As the input frequency is close to the natural frequency of the model slope, the amplification factor gradually increased owing to the resonance while the excitation level was small, and the factor reached its maximum value at the stage with an input acceleration of 1.2 m/s². With the further increase in the input acceleration (the stage with 1.7–5.2 m/s²), although the relationship of the amplification factor in the depth direction was retained, the amplification factor decreased. This is because after the stage of 1.7 m/s², the natural frequency of the model slope changes owing to the reduction in rigidity associated with ongoing plastic deformation of the embankment, and a resonance phenomenon does not occur. Furthermore, if the excitation level increased, the amplification factor of the upper part of the embankment would decrease greatly (ch. 3, 5, 6). In other words, when the input acceleration reaches 5.7 m/s², the amplification factor on the slope side reverses (ch. 3 < ch. 1 < ch. 2), and when the input acceleration reaches 6.2 m/s², an inversion of the factor also occurs on the crest side (ch. 6 < ch. 4 < ch. 5). The reversal of the amplification factor implies that failure occurs in the lower part of the relevant part and the vibration from the depth no longer propagates sufficiently. Considering the deformation/failure mechanism from the viewpoint of reversal of the amplification factor, the failure at the stage is considered to occur with an input acceleration of 5.7 m/s², and a slip surface began to be formed. The excess pore water pressure ratio started increasing from 5.2 m/s², where the inversion of the amplification factor occurs and then shows an upward trend. The inversion phenomenon of the amplification factor and pore water pressure behavior first leads to the formation of the slip,

deformation amount and phreatic surface. The absence of an increase in the excessive pore water pressure ratio in the upper part implies that this portion failed mainly because of the inertial force acting just under the phreatic surface of the top end part.

Figures 10 and 11 show the changes in the amplification factor and excess pore water pressure of Case A, respectively. Although the deformation mode is different, the mechanism leading to the failure is common, and includes collapse due to rigidity reduction associated with the increase of excess pore water pressure ratio and reversal of the acceleration amplification factor occurring at the slip surface.

4 CONCLUSION

In the case where the embankment is in the unsaturated condition, a slip plane is formed along the surface. After that, the slip progressing to the back end of the crown is formed with a delay. The comparison of the experimental results of the unsaturated and saturated fill slopes showed that although the failure mechanism in which the slip surface is formed by the reduction in rigidity is common, the input acceleration at failure and deformation mode are different. When the slip surface is formed and failure occurs, the input acceleration in the unsaturated fill slope is larger and the deformation at same excitation stage is small. This implies that the unsaturated fill slope has a higher earthquake resistance than the saturated fill slope where the conditions other than the groundwater level are the same. In the future, we will conduct a soil–water–air coupled finite deformation analysis and verify the deformation/failure mechanism of a fill slope more precisely.

REFERENCES

Kamai, T., Ohta, H., Ban, Y. and Murao, H. (2013). Landslides in urban residential slopes induced by the 2011 off the Pacific coast of Tohoku earthquake, Studies on the 2011 off the Pacific coast of Tohoku Earthquake, Springer, 103–122.

Nakano, M., Sakai, T., Noda, T. and Asaoka, A. (2010). Soil-water coupled finite deformation analysis of seismic deformation and failure of embankment on horizontal and inclined ground. Proc. of Soil Dynamics and Earthquake Engineering, ASCE. Shanghai, 139‑144.

Murao, H., Nakai, K., Noda, T. and Yoshikawa, T. (2018): Deformation/failure mechanism of saturated fill slopes due to resonance phenomena based on 1G shaking-table tests, Canadian Geotechnical Journal, accepted

Fig. 8 Change of amplification factor in Case B

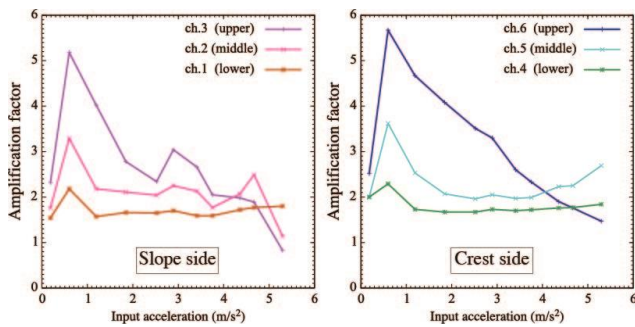Fig. 9 Change of excess pore water pressure in Case B

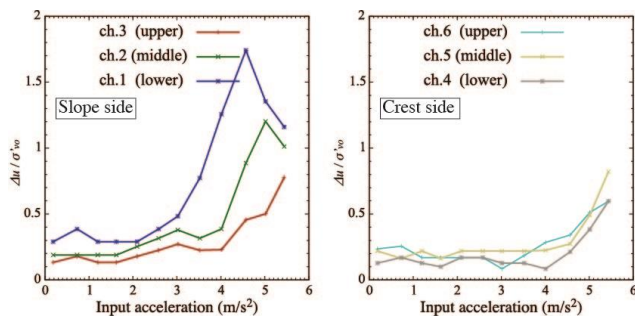Fig. 10 Change of amplification factor in Case A

Fig. 11 Change of excess pore water pressure in Case A

surface (Slip surface 1 in Fig. 5) on the slope side and then another slip surface (Slip surfaces 2 and 3 in Fig. 5) is formed with a delay. On the slope side, the excess pore water pressures at the lower part (ch.9), central part (ch.10), and upper part (ch.11) increase with the excitation stage. In contrast, on the crest side, only the pressure at the lower part (ch.13) and central part (ch.14) increase, and that at the upper part (ch.16) hardly changes. The difference between the slope and crest sides is considered to be the influence of the